Nuclear Engineering and Design 305 (2016) 389–399

Contents lists available at ScienceDirect

Nuclear Engineering and Design

journal homepage: www.elsevier.com/locate/nucengdes

Oxidation effects during corium melt in-vessel retention

V.I. Almyashev [a], V.S. Granovsky [a], V.B. Khabensky [a], E.V. Krushinov [a], A.A. Sulatsky [a], S.A. Vitol [a], V.V. Gusarov [b], S. Bechta [c], M. Barrachin [d], F. Fichot [d], P.D. Bottomley [e,*], M. Fischer [f], P. Piluso [g]

[a] *Alexandrov Scientific-Research Institute of Technology (NITI), Sosnovy Bor, Russia*
[b] *Ioffe Institute, St. Petersburg, Russia*
[c] *Royal Institute of Technology (KHT), Stockholm, Sweden*
[d] *Institut de Radioprotection et de Sûreté Nucléaire (IRSN), St Paul lez Durance, France*
[e] *Joint Research Centre, Institut für Transurane (ITU), Karlsruhe, Germany*
[f] *AREVA GmbH, Erlangen, Germany*
[g] *CEA Cadarache-DEN/DTN/STRI, France*

HIGHLIGHTS

- Corium–steel interaction tests were re-examined particularly for transient processes.
- Oxidation of corium melt was sensitive to oxidant supply and surface characteristics.
- Consequences for vessel steel corrosion rates in severe accidents were discussed.

ARTICLE INFO

Article history:
Received 22 January 2016
Received in revised form 20 May 2016
Accepted 24 May 2016

JEL classification:
C. Material Properties

ABSTRACT

In the in-vessel corium retention studies conducted on the Rasplav-3 test facility within the ISTC METCOR-P project and OECD MASCA program, experiments were made to investigate transient processes taking place during the oxidation of prototypic molten corium. Qualitative and quantitative data have been produced on the sensitivity of melt oxidation rate to the type of oxidant, melt composition, molten pool surface characteristics. The oxidation rate is a governing factor for additional heat generation and hydrogen release; also for the time of secondary inversion of oxidic and metallic layers of corium molten pool.

1. Introduction

Melt oxidation is one of the principal processes influencing the condition of molten corium pool formed in the reactor vessel bottom in the course of PWR, BWR and VVER severe accident progression. Limited mass of water during core re-flood and residual water in the vessel lower head cannot produce enough steam for complete oxidation of fuel, clad and core structural materials (Zr), so the in-vessel corium is considerably suboxidized, i.e. the molten pool contains active reducing agents (U, Zr). Elements of relocated stainless steel of in-vessel structures (Fe, Cr, Ni, Mn, . . .), control rods (Ag, Cd, In, B, C) and reactor pressure vessel (Fe, C, . . .) also belong to this category of redox reaction elements.

On the other hand, during or after the molten pool formation the oxidant can also get access to the pool surface: either water supplied into the vessel or due to the mass exchange between the in-vessel gas atmosphere and steam of the containment. In this case the redox reactions can bring changes to the molten pool structure and composition, as can hydrogen generation and additional heat deposition in the melt. It is therefore necessary to simulate the above-mentioned phenomena in the analysis of melt in-vessel retention (IVR), uncooled vessel failure and hydrogen safety.

In (Khabensky et al., 2003, 2011; Asmolov et al., 2007, 2006; Bechta et al., 2010) the oxidation phenomena of prototypic corium having different compositions and oxidizing atmosphere have been studied in the small-scale experimental facilities. In Sulatsky et al. (2013) results of these studies are analyzed. It was established that practically in all cases the oxidation is in the starvation mode, i.e. its rate is limited by the flow rate of oxidant supply to the melt surface. It is noted that surface oxidic crust provides an additional diffusion barrier and reduces the oxidation rate. References Asmolov et al. (2007) and Sulatsky et al. (2013) also give some

---

* Corresponding author. Tel.: +49 7247 951 364; fax: +49 7247 951 593.
E-mail address: paul.bottomley@ec.europa.eu (P.D. Bottomley).

http://dx.doi.org/10.1016/j.nucengdes.2016.05.024
0029-5493/

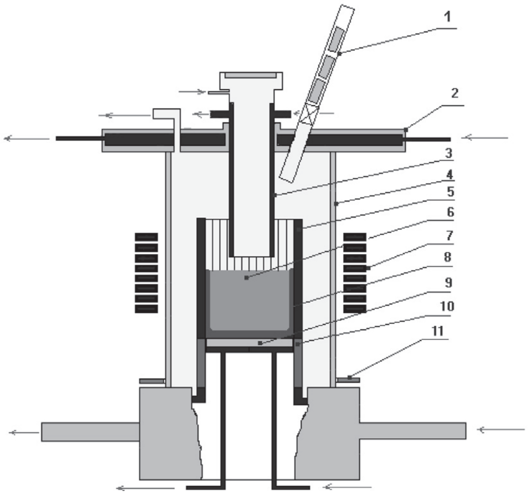

Fig. 1. Rasplav-3 induction furnace schematics. (1) Port for metal introduction; (2) furnace cover; (3) pyrometer shaft flushed with argon; (4) quartz tube; (5) cold crucible sections; (6) corium melt; (7) inductor; (8) crust; (9) bottom calorimeter; (10) water-cooled electromagnetic screen; (11) shield of collector unit.

examples of secondary inversion of oxidic and metallic layers after sufficient oxidation of corium molten pool when an initial bottom U and Zr-rich metallic melt has occurred.

This paper gives further analysis of previous experimental data (Sulatsky et al., 2013) and new data about the effect of oxidic crusts.

2. Experimental

Experimental studies of the prototypic corium oxidation phenomena, which are discussed in this paper, were conducted on the Rasplav-3 tests facility of the RASPLAV platform in NITI within the ISTC METCOR-P project and OECD MASCA program. All experiments except MCP-6 used the technology of induction melting in a cold crucible. The induction furnace schematics is given in Fig. 1. In MCP-3 the bottom calorimeter (Fig. 1, item 9) was replaced by the water-cooled reactor vessel steel specimen. In experiments with steam used as the oxidant (MCP-3, MCP-6, MCP-7, MA-9) a practically identical gas-aerosol system was used, which is shown in Fig. 2. The gas-aerosol system schematics in the experiment with air (MA-7) is shown in Fig. 3.

In experiments with oxidic or oxidic-metallic melt (MCP-3, MCP-7, MA-7, MA-9) the initial corium oxidation index is approximately C-30 (that is 30% of the initial inventory of Zr (in moles) is oxidized to ZrO_2), and uranium–zirconium ratio $(U/Zr)_{at} \approx 1.2$. Table 1 in the Discussion (Section 3) summarises the conditions of the experiments together with major results.

2.1. Experiment MCP-3

Experiment MCP-3 was conducted within the METCOR-P project. The molten pool bottom lay on the flat surface of a cylindrical steel specimen inside the water-cooled crucible of induction furnace. The arrangement was the same as in experiments on the interaction between the suboxidized corium melt and reactor vessel steel (Bechta et al., 2004, 2006). The molten pool was produced in an argon atmosphere on the surface of specimen, the bottom of which was cooled with water. As a result of steel–melt interaction, the liquid–solid interaction zone (IZ) was formed at the specimen surface, which was separated from the melt by oxidic crust; its main components were Fe, U and Zr. At this stage (stage A) the experiment practically repeated experiment MC6 of METCOR (Bechta et al., 2004).

After that, by shifting the electromagnetic screen and crucible and reducing power deposition into the melt the massive oxidic crust was formed on the steel specimen surface; it was made in parallel with a substantial steel specimen temperature reduction (stage B). After that the above-melt argon atmosphere was replaced with steam. This atmosphere was maintained by steam supply with the flow-rate of approx. 400 g/h (111 mg/s). During 30 min (stage C) the melt was oxidized in the crust-free regime, excluding the startup and finish periods. During this, no water condensate was observed in the condenser installed in the gas line (see item 6 in Fig. 2). The massive oxidic crust on the steel surface prevented the IZ oxidation during stage C. Later, approximately within 1 h 20 min (stage D), crust thickness on the steel specimen surface was reduced to the value, from which the IZ oxidation process was started and completed (stage E). At this stage a part of the supplied steam did not interact with melt; it was evacuated from the furnace into the condenser (see items 5 and 6 in Fig. 2).

Fig. 4 illustrates oxidation processes at stages C and E by the corresponding correlations of hydrogen release versus time determined from the steam oxidation of the reducing agent components. Correlations (1) illustrate oxidation process at stages C and E.

$$U/Zr + 2H_2O = UO_2/ZrO_2 + 2H_2 \tag{1}$$

For stage C the hydrogen release rate was 9.9 mg H_2/s, and for stage E – 5 mg H_2/s. Taking into account the melt surface area (crucible inner diameter was 70 mm) the oxygen release rate per unit surface area is 0.26 for stage C and 0.13 mg $H_2/(cm^2\ s)$ for stage E. The corresponding values of the steam-melt mass interaction rate are 2.34 and 1.17 mg $H_2O/(cm^2\ s)$.

In MCP-3 it was difficult to determine concentration of H_2 which flowed out from the furnace in the carrier gas (N_2). The same problem was with the water condensate rate measurement. Therefore, the calculations of mentioned rates were made by measuring oxygen consumption for the oxidation of reducing agents in the corium melt and IZ. The methodology is explained in detail in Khabensky et al. (2011). This work also provides an insight into the melt surface condition. It follows that at brief time intervals in the beginning and in the end of stage C, also in the end of stage E, the melt surface was covered with crust. Therefore, for most of the time during both stages, the oxidic crust was not present on the melt surface.

2.2. Experiment MA-9

Experiment MA-9 (Asmolov et al., 2007) was conducted within the MASCA program. Initially the molten pool was established in the argon atmosphere (crucible inner diameter the same as in MCP-3 – 70 mm). Stainless steel was added (Kh18N10T), its mass fraction in the melt was 0.1. After reaching the state of equilibrium resulting from the component partitioning between the suboxidized corium and SS melts, the two-liquid molten pool was formed with the oxidic liquid in a surface position. After that steam was supplied to the above-melt atmosphere at a flow-rate of approx. 800 g/h (222 mg/s); the melt oxidation was going on for approx. 20 min. The analysis of post-experimental ingot revealed metallic layer was in the surface position, which indicated the inversion of oxidic and metallic liquids in the course of melt oxidation.

In MA-9 the flow rate of steam spent on the melt oxidation was calculated from the difference between the supplied steam and measured condensate mass at the furnace exit taking into account water collected by the filters. Fig. 5 shows the experimental data, according to which the melt oxidation rate was approximately steady, the interaction rate of the steam with the melt was 0.11 g H_2O/s, and the rate per unit surface area was 2.92 mg $H_2O/(cm^2\ s)$. In Sulatsky et al., 2013 the posttest analysis has shown